Intercomparison of Pandora Stratospheric NO$_2$ Slant Column Product with the NIWA M07 NDACC Standard

Travis N. Knepp[1,2], Richard Querel[3], Paul Johnston[3], Larry Thomason[2], David Flittner[2], and Joseph M. Zawodny[2]

[1]Science Systems and Applications Inc., Hampton, VA, 23666 United States
[2]NASA Langley Research Center, Hampton, VA, 23681 United States
[3]National Institute of Water and Atmospheric Research, Lauder, Central Otago, New Zealand

Correspondence to: Travis N. Knepp
(travis.n.knepp@nasa.gov)

Abstract. In September 2014 a Pandora multi-spectral photometer operated by the SAGE-III project was sent to Lauder, New Zealand to operate side-by-side with the National Institute of Water and Atmospheric Research's (NIWA) Network for Detection of Atmospheric Composition Change (NDACC) standard zenith slant column NO$_2$ instrument to allow intercomparison between the two instruments, and evaluation of the Pandora unit as a potential SAGE-III validation tool for stratospheric NO$_2$.

5   This intercomparison spanned a full year, from September 2014 – September 2015. Both datasets were produced using their respective native algorithms using a common reference spectrum (i.e. 12:00 on 26-February 2015). Throughout the entire deployment period both instruments operated in a zenith-only observation configuration. Though conversion from slant column density (SCD) to vertical-column density is routine (by application of an air mass factor), we limit the current analysis to SCD only. This omission is beneficial in that it provides a strict intercomparison of the two instruments and the retrieval algorithms

10 as opposed to introducing an AMF-dependence in the intercomparison as well. It was observed that the current hardware configurations and retrieval algorithms are in good agreement (R > 0.95). The detailed results of this investigation are presented herein.

1   Introduction

The Stratospheric Aerosol and Gas Experiment (SAGE) missions have provided a legacy of high-quality solar occultation

15 measurements of stratospheric ozone and aerosol for over 3 decades (Chu and McCormick, 1979, 1986; Damadeo et al., 2013; Cisewski et al., 2014). SAGE-III/Meteor, operated aboard the Russian Meteor-3M platform between February 2002 and March 2006. An updated version of this instrument was integrated into the International Space Station (ISS) in March 2017 with routine observations expected to start in April. As with any new instrument, a significant post-launch activity is planned to validate the accuracy and precision of the data products, and provide validated datasets to end users. While the key SAGE-III

20 species measurements are validated using well-known and characterized instruments, one important product remains difficult to measure: NO$_2$. NO$_2$ is important due to its role in partitioning stratospheric odd hydrogen, providing a chemical pathway for conversion of ozone-destroying species to their reservoir forms (e.g. halogen species as discussed by Wennberg et al. (1994)),

Atmospheric
Measurement
Techniques
Discussions

and may be responsible for up to 70 % of the stratospheric ozone loss (Crutzen, 1970; WMO, 1985; Seinfeld and Pandas, 1998; Chartrand et al., 1999; Portmann et al., 1999).

Due to the unique viewing geometry of SAGE-II and the rapid variability of NO_2 across the solar terminator, NO_2 measurements from SAGE-II proved to be challenging. SAGE-III/Meteor NO_2 is often validated using measurements from other space-based instruments that generally do not fully match the SAGE viewing geometry, location and/or time. While a chemistry model can correct for some of these differences, generally these comparisons leave significant questions regarding the NO_2 data quality.

An alternative method that provides some corroboration to the SAGE-III measurement quality is comparison with ground-based Differential Optical Absorption Spectroscopy (DOAS, e.g. Platt and Stutz, 2008) or Fourier Transform Spectroscopy (FTS, e.g. Wang et al., 2010) measurements of the column NO_2 using zenith-looking instruments that measure scattered light across the ultra-violet and visible wavelengths. These observations can be used to infer, among other species, column NO_2 as a function of solar zenith angle (SZA). Zenith-viewing observations when SZA $\approx 90°$ are analogous to solar occultation measurements of NO_2. However, observation of stratospheric NO_2 is challenging at many locations due to the preponderance of tropospheric NO_2 from anthropogenic sources. Therefore, measurement sites that are in locations that are considered "background-level" are advantageous.

The National Institute of Water and Atmospheric Research (NIWA) Lauder, New Zealand site provides the desired background-level conditions. The Lauder group has a long history of providing high-quality observations (McKenzie and Johnston, 1982; McKenzie et al., 1992), and is generally considered a standard for stratospheric NO_2 observations. Data collected at the Lauder site have been used to infer data quality for SAGE II NO_2 and were used to identify and help correct a time-dependent error in those observations (Damadeo et al., 2013). For the new SAGE-III mission, observations by the NIWA instrument will be useful for understanding NO_2 data quality. However, since the challenges of making space-based measurements is often latitude dependent, a single site will not provide all the corroborative data needed to make a robust assessment of data quality. As a result, the SAGE-III group has acquired a Pandora unit (Herman et al., 2009; Tzortziou et al., 2015) with the hope of using it as a portable system for providing corroborative data that can be deployed at sites of opportunity, for instance low latitudes, throughout the SAGE-III/ISS mission. To date, Pandoras have not established a record for measuring NO_2 where the column is dominated by the stratosphere rather than a polluted troposphere so an evaluation of the capabilities of this instrument in this regard is necessary. Herein, we report the results of a comparison of observations by the NIWA M07 instrument and the SAGE-III Pandora unit when operated side-by-side between September 2014 and September 2015 at the NIWA facility in Lauder, New Zealand.

2 Instrumentation

2.1 LaRC Pandora

Pandora is a sun-viewing spectrometer that was initially developed for validation of the Ozone Monitoring Instrument (OMI) aboard the Aura satellite (Herman et al., 2009; Lamsal et al., 2014; Tzortziou et al., 2015), and has proven to be sensitive

Atmospheric
Measurement
Techniques
Discussions

Gas	Instrument	Cross Section	T (K)	λ Range (nm)
O$_3$	Pandora	Daumont et al. (1992); Malicet et al. (1995)	225	300 – 330
	M07	Brion et al. (1993)	218	300 – 330
NO$_2$	Pandora	Vandaele et al. (1998)	220	400 – 485
	M07	Vandaele et al. (1998)	220	400 – 485
O$_4$	Pandora	Smith et al. (2001)	262	400 – 454.42
	Pandora	Newnham and Ballard (1998)	262	454.43 – 485
	M07	Newnham and Ballard (1998)	262	400 – 454.42

Table 1. Relevant cross-section details for the two instruments under study. Species that required multiple cross-section sources to cover the required wavelength range (e.g. O$_4$) have multiple cross sections listed and their respective wavelength domains.

to fluctuations in boundary layer NO$_2$ over short time periods (Knepp et al., 2015). Due to Pandora's potential for retrieving stratospheric gas column densities (i.e. operating in zenith orientation during twilight hours) it has been evaluated as a potential validation instrument for the SAGE-III mission.

A detailed description of the instrument has been provided by Herman et al. (2009). Briefly, the Pandora model used in the

5   current study consisted of: 1. an optical head (mounted on a two-axis tracker capable of moving through 360º azimuth and 180º zenith) containing filter wheels for controlling polarization and radiant flux; 2. a single-strand, multi-mode fiber-optic cable with 400 μm core diameter and numerical aperture of 0.22 to transmit photons to the spectrometer; 3. a temperature stabilised Avantes spectrometer (model number ULS2048x64, 280 – 525 nm) with a 50 μm slit, focal length of 75 mm, and resolution on the order of 0.6 nm; 4. laptop computer for instrument control and data logging. The improved optics and spectrometer

10   of this model enabled the instrument to record solar spectra from lunar reflectance and scattered radiation, thereby enabling acquisition of twilight spectra for estimating the slant-column density (SCD) stratospheric component and potential for vertical profiling of select species.

The Pandora retrieval algorithm was previously described in Herman et al. (2009) and Tzortziou et al. (2015), with relevant cross-section details presented in Table 1. Briefly, spectral fitting is performed using laboratory-measured absorption cross

15   sections and implement shift-squeeze functions to fit the observed spectra with the solar reference spectrum's Fraunhofer line structure (for zenith observations an instrument-observed solar-reference spectrum was used from the spectrum recorded at 12:00 (local time) on 26-February 2015), with a fourth-order polynomial applied for removal of aerosol and Rayleigh scattering effects.

Though Pandora was developed to operate in a Sun-tracking mode and has undergone numerous revisions to allow data

20   collection in sky (i.e. scattered irradiance) and moon observation modes, in this study the Pandora only operated in the zenith-observation mode to allow direct intercomparison with the NIWA instrument.

Atmospheric
Measurement
Techniques
Discussions

2.2 NIWA spectrometer

The NIWA instrument (M07) is a zenith-oriented instrument used for measuring stratospheric slant column NO_2. M07 is the current instrument contributing to the continuous time series of stratospheric NO2 from Lauder that started in 1980, and is part of the Network for Detection of Atmospheric Composition Change (Hofmann et al., 1995; Roscoe et al., 1999). The

5 M07 instrument has been described previously (McKenzie and Johnston, 1982; McKenzie et al., 1992; Hofmann et al., 1995). Briefly, M07 is a Czerny-Turner monochromator (320 mm focal length, $\approx$0.8 nm resolution, F/5 entrance field of view, 1 mm wide slit) with a bi-alkali photocathode photomultiplier detector. The scanning mechanism has been modified to provide fast scanning with a long lifetime and smooth wavelength motion. The instrument is mounted in a temperature controlled cabinet on a rotating table following the line of the sun-zenith plane and a Glan-Thompson polariser is used in front of the entrance silt

10 to provide polarised zenith measurements. Similar to the Pandora, the cross sections used for retrievals are listed in Table 1.

3 Mode of operation and location

The Pandora unit was deployed to the NIWA station in Lauder, Central Otago, New Zealand (45.038 S, 169.68 E, 370 m ASL) to run side-by-side with the NIWA-operated M07 spectrometer. Both instruments performed retrievals using a common reference spectrum (collected on 26-February, 2015 12:00 local time) as observed by the respective instruments. It is worth

15 noting that, other than the Pandora's fixed zenith observation state) both instruments were operated in their normal states, not in a customized operation mode, and both used their standard retrieval algorithms.
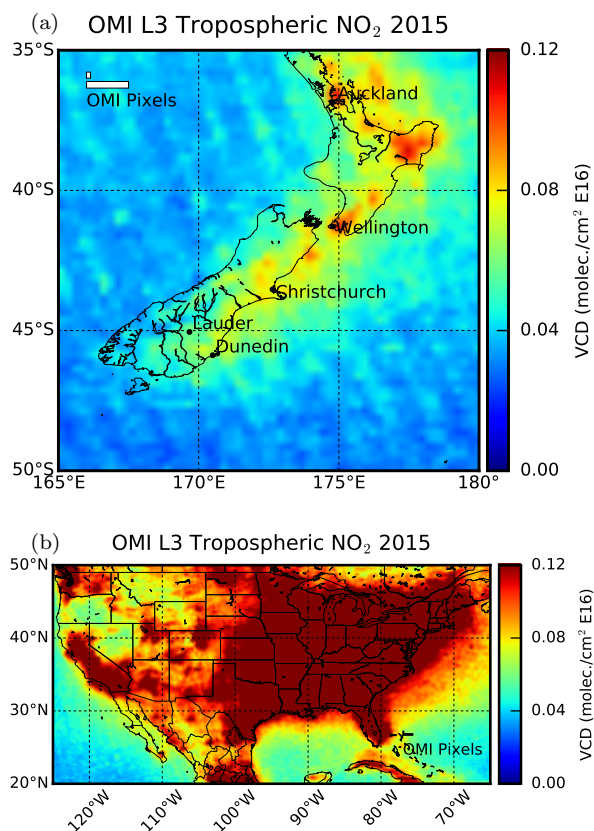
New Zealand is generally an atmospherically clean environment, with pollution levels that can be considered as background level (e.g. approximately an order of magnitude below urban centers in the continental United States). As a point of reference, NO_2 retrievals over New Zealand and the continental United States from the OMI (Level 3, version 3 algorithm) are presented

20 on the same scale in Figs. 1 and 2. It is observed that aside from some western states (e.g. Nevada and Oregon), the U.S. rarely experiences similar clean conditions as New Zealand. Furthermore, Fig. 2 displays a downward trend in overall column NO_2 over the Chemistry and Physics of the Atmospheric Boundary Layer Experiment (CAPABLE) station located at NASA's Langley Research Center in Hampton, VA (37.103 N, -76.387 E, 5 m ASL) that is being driven by a decreasing tropospheric column, while NO_2 over Lauder has remained consistent since 2005. There is no corresponding change in stratospheric NO_2

25 for either site.

Statistics describing the variability in NO_2 over both sites were broken into three categories (total-column, stratospheric and tropospheric contributions) and are presented in Table 2. The statistics presented in Table 2 are similar for both sites when scaled according to corresponding column density (i.e. despite the total-column standard deviation being significantly different for both sites the relative error ($\sigma/\overline{x}$) remains similar). Despite these similarities, the tropospheric variability remains different

30 for the two sites indicating a higher degree of variability over the continental US. The tropospheric contribution and variability remains significantly higher over CAPABLE as compared to Lauder with approximately 55.7 % of the NO_2 column residing in the troposphere over the CAPABLE site, and only 13.5 % over Lauder. These differences are driven by the ubiquity of local sources in the eastern United States as compared to central New Zealand.
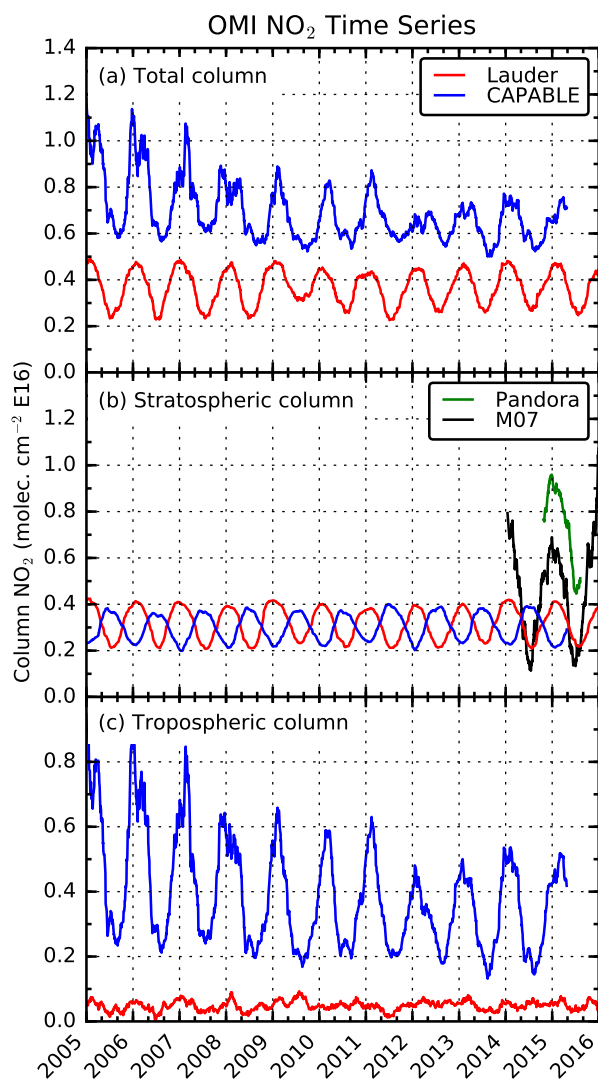
Atmospheric
Measurement
Techniques
Discussions

Figures 1 and 2 and Table 2 demonstrate that not only is the NO_2 column significantly higher over the continental US, but the Lauder column is dominated by the stratospheric contribution. One effect of differing source strengths is seen in Fig. 2. Being in different hemispheres, the two sites should be approximately six months offset in their seasonal cycle, though the total-column time series shows the two sites are in phase. However, the stratospheric contribution for the two sites (panel

5   b) remained approximately six months out of phase as expected. This can be explained by the difference in tropospheric and stratospheric chemistry. Under normal, moderately-polluted conditions, tropospheric chemistry is sufficiently perturbed to force the tropospheric NO_2 column density out of phase with the stratosphere. This shows up in the data as an approximately six month offset. Since the northern hemisphere site is dominated by tropospheric NO_2 (as shown in Fig. 2 and Table 2), and the southern hemisphere site has significantly less tropospheric contribution, the two sites were in phase with one another in

10   the total-column panel.

Since Lauder provides a clean, background-level, environment with few local or regional anthropogenic emission sources, it provides ideal conditions for observation of stratospheric species and evaluation of the Pandora system for detecting stratospheric NO_2 and as a possible validation tool for current and upcoming satellite missions that focus on stratospheric chemistry.

Figure 1. Annual average for OMI NO$_2$ (L3, v3.0) maps over New Zealand and North America. OMI pixel sizes (nadir and swath edge) are represented by the white boxes within each panel. For comparison purposes, both plots were put on the same color scale.

Figure 2. Time-series plots for total- (a), stratospheric- (b), and tropospheric-column (c) NO_2 data products from OMI (L3, v3.0) over Lauder (red) and CAPABLE (blue). OMI data were filtered to remove cloud fractions greater than 20 % and overpasses greater than 50 km from the site. Pandora (green) and M07 (black) data presented in panel b are slant-column densities.

4 Intercomparison

Pandora and M07 data were filtered to remove points where the retrieval uncertainty was greater than 10 % of the retrieved value followed by resampling to five-minute means to allow direct, temporally-aligned, intercomparisons. For plotting purposes,

Parameter	Lauder	CAPABLE
Total-column ($\overline{x}$)	0.37	0.70
Total-column (σ)	0.08	0.14
Total-column ($\sigma/\overline{x}$)	0.21	0.19
Stratosphere ($\overline{x}$)	0.32	0.31
Stratosphere (σ)	0.07	0.06
Stratosphere ($\sigma/\overline{x}$)	0.21	0.19
Stratospheric Fraction (%)	86.5	44.3
Troposphere ($\overline{x}$)	0.05	0.39
Troposphere (σ)	0.01	0.17
Troposphere ($\sigma/\overline{x}$)	0.29	0.45
Tropospheric Fraction (%)	13.5	55.7

Table 2. Statistics regarding stratospheric and tropospheric contribution and variability of NO_2 as observed by OMI. All units are molec cm^{-2} E16.

some datasets were smoothed via a rolling mean (e.g. to remove higher-frequency fluctuations). Unless otherwise noted, all intercomparisons and analyses were carried out using 5 min averaged data.

4.1 Aggregate analysis

An aggregate analysis was performed on the resampled data by binning the SCD according to SZA for a visual evaluation of
5   correlation as seen in Fig. 3. It is observed that the correlation is generally poor during pre-sunrise/twilight hours (i.e. when SZA>92.5°), but improves with decreasing SZA where it peaked at 80-85°. Within each sub-panel of Fig. 3 the data were color coded to correspond to the SZA range within each sub-panel and provide insight into how the short-term change in SZA influenced correlation. As an example, in panel a it is observed that data collected at higher SZA (red-shaded points) were further from the one-to-one line than data collected at lower SZA (blue-shaded points). Analogously, it is observed in panels
10   e-g that as SZA decreased, so too did the degree of correlation. Therefore, we can conclude that the Sun's zenith angle played a role in the degree of agreement between the two instruments, though this dependence cannot be separated from day-to-day chemical variability.

It remains clear that the two instruments had strikingly good agreement for zenith angles greater than 70°, as supported by Fig. 3 and Table 3. Below 70° the correlation dropped rapidly (by almost fifteen percentage points between bins). However,
15   when considering data collected within the SZA range most relevant to stratospheric retrievals (i.e. (80,92.5]) the mean percent difference remained below 10 %, with R^2 >0.95. From a satellite-validation perspective, this bodes well for future validation efforts of stratospheric NO_2 as >95 % of the inter-instrument variability is accounted for without further correction at zenith angles most relevant to stratospheric observation.
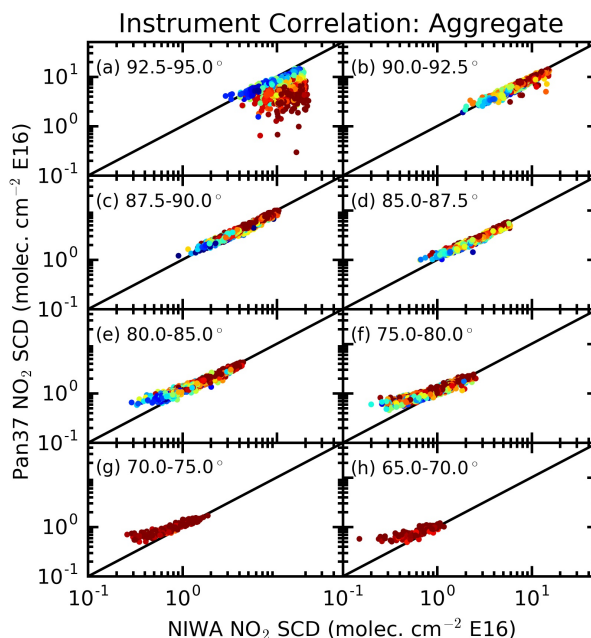
Atmospheric
Measurement
Techniques
Discussions

N	Pandora ($\bar{x}$)	M07 ($\bar{x}$)	Diff. ($\bar{x}$)	Diff. (σ)	% Diff.	Ratio ($\bar{x}$)	Slope	Intercept	R^2	SZA Range
1135	6.488	11.648	-5.160	4.00	44.3	0.602	0.226	3.860	0.128	(92.5,95.0]
848	7.072	7.933	-0.861	0.915	10.9	0.907	0.820	0.569	0.933	(90.0,92.5]
1208	4.470	4.767	-0.297	0.463	6.2	0.955	0.866	0.340	0.955	(87.5,90.0]
752	2.914	3.025	-0.111	0.289	3.7	0.991	0.850	0.344	0.958	(85.0,90.0]
1660	1.895	1.855	0.040	0.199	2.2	1.076	0.841	0.336	0.960	(80.0,85.0]
1260	1.223	1.088	0.135	0.149	12.4	1.214	0.787	0.367	0.920	(75.0,80.0]
235	1.003	0.848	0.155	0.129	18.3	1.289	0.737	0.378	0.899	(70.0,75.0]
151	0.806	0.649	0.157	0.108	24.3	1.323	0.702	0.351	0.752	(65.0,70.0]

Table 3. Summary of aggregate statistics for the Pandora/NIWA intercomparison using the standard algorithms and parameters for each instrument. Differences and ratios are relative to the NIWA instrument (i.e. Pandora - M07, Pandora/M07). Statistics were generated using data that were resampled to 5 min means; no further smoothing or binning was applied.

Season	N	Pandora ($\bar{x}$)	M07 ($\bar{x}$)	Diff. ($\bar{x}$)	Diff. (σ)	% Diff.	Ratio ($\bar{x}$)	Slope	Intercept	R^2	SZA Range
Summer	694	6.957	12.735	-5.778	4.056	-45.4	0.582	0.181	4.651	0.071	(92.5,95.0]
Winter	258	4.972	8.129	-3.157	2.716	-38.8	0.660	0.140	3.835	0.045	
Summer	513	7.744	8.795	-1.051	0.880	-11.9	0.888	0.831	0.440	0.926	(90.0,92.5]
Winter	202	4.839	5.124	-0.285	0.577	-5.6	0.961	0.829	0.593	0.917	
Summer	729	4.837	5.269	-0.432	0.477	-8.2	0.928	0.870	0.252	0.947	(87.5,90.0]
Winter	284	3.139	3.103	0.036	0.239	1.2	1.025	0.932	0.248	0.960	
Summer	469	3.138	3.340	-0.202	0.271	-6.1	0.952	0.870	0.233	0.952	(85.0,87.5]
Winter	167	1.994	1.849	0.145	0.162	7.8	1.106	0.900	0.330	0.953	
Summer	1044	2.031	2.050	-0.020	0.198	-1.0	1.025	0.839	0.311	0.954	(80.0,85.0]
Winter	366	1.322	1.135	0.188	0.124	16.5	1.224	0.902	0.298	0.943	
Summer	872	1.254	1.146	0.108	0.146	9.5	1.170	0.774	0.368	0.925	(75.0,80.0]
Winter	227	0.906	0.672	0.234	0.106	34.8	1.439	0.891	0.307	0.868	
Summer	173	1.019	0.878	0.141	0.132	16.0	1.259	0.702	0.403	0.905	(70.0,75.0]
Winter	36	0.736	0.521	0.215	0.104	41.3	1.516	0.782	0.328	0.775	
Summer	132	0.798	0.639	0.158	0.105	24.8	1.318	0.701	0.349	0.752	(65.0,70.0]
Winter	4	0.670	0.445	0.225	0.143	50.4	1.951	0.601	0.402	0.693	

Table 4. Summary of seasonal statistics for the Pandora/NIWA intercomparison. Similar to Table 3.

Atmospheric
Measurement
Techniques
Discussions

Figure 3. Correlation plots for data collected by the Pandora and M07 instruments. Data were resampled to five-minute averages, and color coded according to SZA within the specified bin range (i.e. red colors represent the upper-SZA limit, blue represent the lower-bounds for each sub-panel).

The decreased correlation at lower SZA's (i.e., as the Sun approaches solar noon) was driven by an apparent offset in the Pandora retrieval at lower SCD's ($\approx 0.55 \times 10^{16}$ molec cm^{-2}) where Pandora seems to lose sensitivity and accuracy, as seen in panels e-h of Fig. 3. A similar "tailing" effect due to decreased sensitivity was observed by Knepp et al. (2015) when comparing Pandora NO$_2$ VCD's to in-situ observations and is likely due to the instrument's accuracy limit ($\approx 0.3 \times 10^{16}$ molec cm^{-2} as stated in (Herman et al., 2009)). Therefore, 0.55×10^{16} molec cm^{-2} is considered to be the lower-limit of detection for the current instrument. However, due to the M07's larger slit width and longer focal length, it has more throughput and greater sensitivity than the Pandora. This allows M07 to continue making reliable measurements up to SZA of 95°.

4.2 Seasonal dependence

To better understand seasonal variability, the data were broken into two major seasons: austral summer (DJFM) and austral winter (JJAS). Seasonal-correlation plots were generated (Fig. 4), and showed nearly identical behavior as the aggregate (Fig. 3), though most of the tailing behavior was isolated to winter conditions.

SCD and statistical time series plots (Fig. 5) were generated to evaluate the seasonal dependence of both instruments and the inter-instrumental statistics over the year-long operation period. The SCD time series was generated by first binning the data by

Atmospheric
Measurement
Techniques
Discussions

Open Access

EGU

SZA followed by calculating daily means, which were then smoothed via a 7-day rolling mean. Statistical time series presented in panels e-af were generated by resampling each dataset to 5 min averages (i.e., forcing both datasets onto a common date/time index) followed by calculation of the specified statistic on a day-by-day basis, which was then smoothed via a 7-day rolling mean.

5   Both instruments displayed the expected diurnal (elevated at large SZA, reduced at smaller SZA) and seasonal (elevated NO_2 in austral summer (DJFM), followed by reduced levels in winter (JJAS)) trends in NO_2 SCD (see also Table 4). This is in agreement with the expected diurnal behavior (Fishman et al., 2008) and the observed satellite seasonality (Fishman et al. (2008) and Fig. 2).
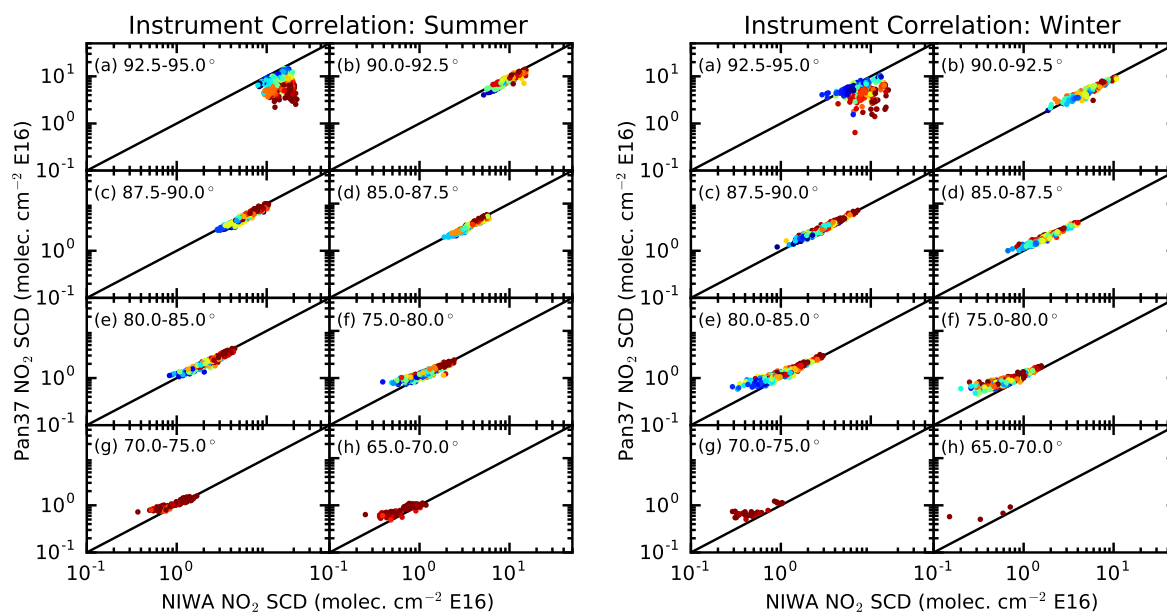
Inter-instrumental statistics and seasonal dependence were further evaluated. It was observed that the two products tended to

10   have good agreement throughout the year (generally with ± 10 %, see Table 4 and Fig. 5 panels m-p), with maximal differences at extreme SZAs (i.e. $>2.5°$ below the horizon, panel a) or at extreme-low NO_2 (i.e. below the Pandora's sensitivity cutoff, as demonstrated in the tailing behavior of Fig. 3). Further, no seasonal dependence on R^2 was observed as R^2 remained high throughout the year (>95 %, Table 4 and Fig. 5 panels m-p).

Other statistics presented in Table 4 and Figure 5 show a slight seasonal dependence in the measured values. An interesting

15   seasonal and SZA dependence was observed in the ratio and slope data in Table 4 in that the wintertime ratios and slopes were always larger than their summertime counterparts (excluding the pre-sunrise data), and can be most clearly seen in the ratio and difference data in Fig. 5. Ideally, the ratio and inter-instrument offset would remain constant regardless of season, though this was not observed. What is observed is a disproportionate increase in the Pandora-measured SCD (i.e. increasing difference and ratio) from summer to winter compared to M07. Even after removing data where SCD<1x10^{16} the wintertime ratios remain

20   disproportionately high, therefore this cannot be attributed to Pandora's low-SCD trailing affect. While the source of this seasonal dependence remains unknown, the observed seasonality changed slow enough that the correlations and regressions were not significantly influenced.

5   Conclusions

The Pandora instrument was collocated with an NDACC-standard instrument (M07 spectrometer) at the NIWA station in

25   Lauder, New Zealand over the period of one year. Spectra from each instrument were processed on separate algorithms to calculate the NO_2 SCD throughout the day, but with a focus on twilight periods. We showed that the two instruments and algorithms were well correlated ($R^2 >0.95$) throughout the entire intercomparison period, and that time of year had minimal impact on the results. Further, it was shown that, within a specified SZA bin, a change in SZA influenced the correlation (e.g. Figs. 3 and 4).

30   The Pandora instrument was shown to have a fundamental limitation due to so-called tailing effects, which are a product of the spectrometer's signal-to-noise, and the overall system's precision and accuracy limits. Therefore, Pandora systems may experience sensitivity problems under either extreme-clean conditions (though the authors cannot identify a region that may be cleaner than southern New Zealand), or winter time near solar noon; neither of which influence twilight retrievals. However,

Figure 4. Correlation plots for data collected by the Pandora and M07 instruments broken into austral summer/winter. Similar to Fig. 3, data were resampled to five-minute averages, and color coded according to SZA within the specified bin range
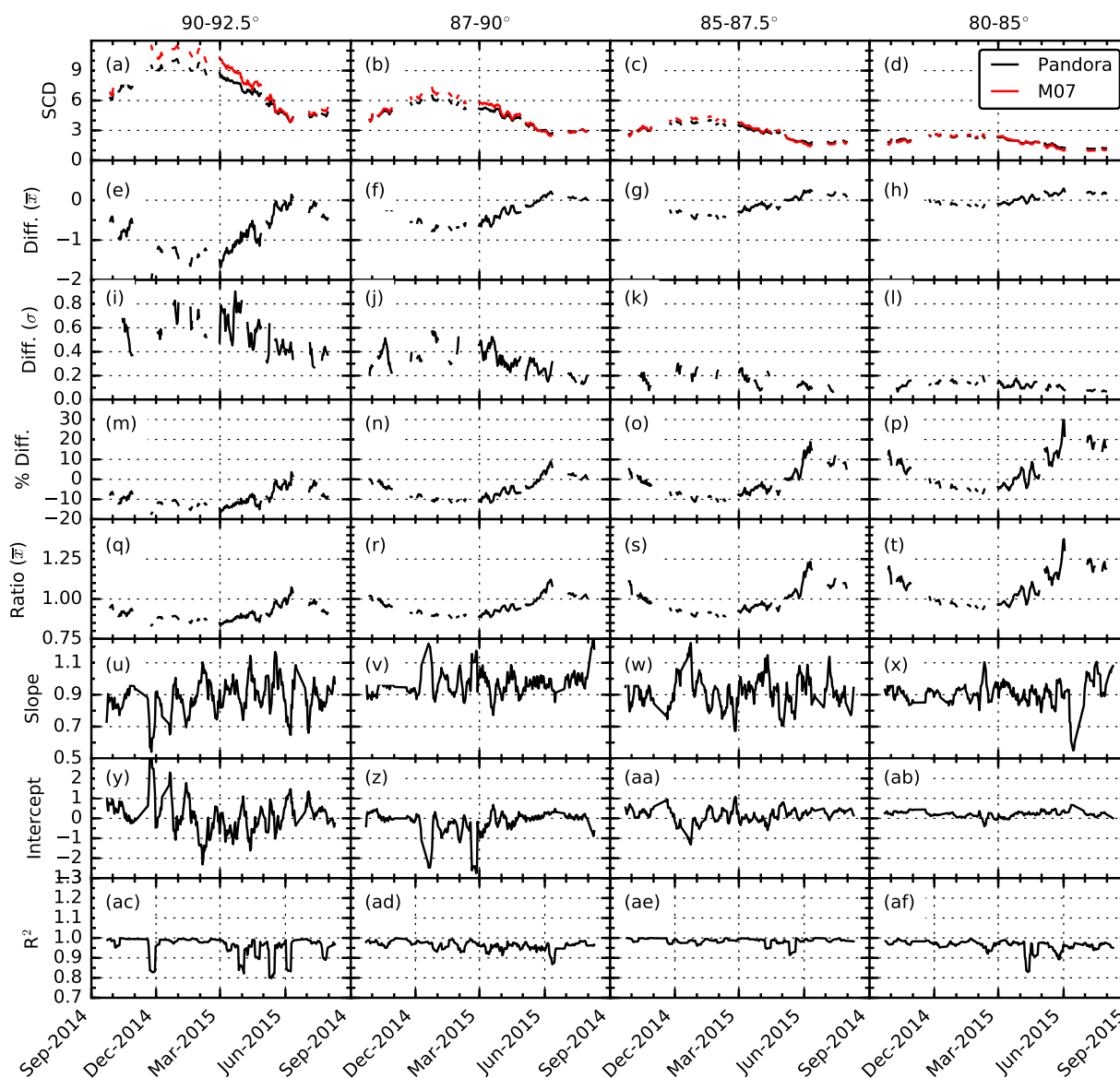
the Pandora instrument may prove useful for SAGE-III validations for SZA observations near 90° and possibly down to 85°. Lower SZA's may not be accessible due to inconsistent curvature from site to site. The SAGE-III project plans on deploying Pandora to sites of interest (ideally low-latitude, tropospherically-clean environments) with balloon-launching capabilities for ongoing validation work. Due to Pandora's portability the instrument can be quickly deployed in response to events of interest

5 (e.g. volcanic eruptions).

6   Data availability

All data used within the current study and all code are available from the authors upon request. OMI data are available from the OMI team via http://avdc.gsfc.nasa.gov/index.php?site=2045907950.

Competing interests.   The authors declare they have no conflict of interest.

Atmospheric
Measurement
Techniques
Discussions

Figure 5. Time series for NO_2 SCD and daily statistics binned by solar-zenith angle. Data were smoothed by a seven-day rolling mean. Panel descriptions: a-d: SCD for both instruments broken up by SZA; e-h: mean SCD difference (Pandora - M07); i-l: standard deviation of differences; m-p: percent SCD difference; q-t: SCD ratio (Pandora/M07); u-x: line of best fit slope (Pandora vs. M07); y-ab: line of best fit intercept; ac-af: R^2 coefficient of correlation.

Atmospheric
Measurement
Techniques
Discussions

References

Brion, J., Chakir, A., Daumont, D., Malicet, J., and Parisse, C.: High-Resolution Laboratory Absorption Cross-Section of O3 - Temperature Effect, Chemical Physics Letters, 213, 610–612, doi:10.1016/0009-2614(93)89169-I, 1993.

Chartrand, D., de Grandpre, J., and McConnell, J.: An introduction to stratospheric chemistry: Survey article, Atmosphere-Ocean, 37, 309–

5   367, Canadian Middle Atmosphere Modelling Project Summer School, Cornwall, Canada, Aug, 1997, 1999.

Chu, W. and McCormick, M.: Inversion of Stratospheric Aerosol and Gaseous Constituents from Spacecraft Solar Extinction Data in the 0.38-1.0-μm Wavelength Region, Applied Optics, 18, 1404–1413, doi:10.1364/AO.18.001404, 1979.

Chu, W. and McCormick, M.: SAGE Observations of Stratospheric Nitrogen-Dioxide, Journal of Geophysical Research-Atmospheres, 91, 5465–5476, doi:10.1029/JD091iD05p05465, 1986.

10   Cisewski, M., Zawodny, J., Gasbarre, J., Eckman, R., Topiwala, N., Rodriguez-Alvarez, O., Cheek, D., and Hall, S.: The Stratospheric Aerosol and Gas Experiment (SAGE III) on the International Space Station (ISS) Mission, in: Sensors, Systems, and Next-Generation Satellites XVIII, edited by Meynart, R and Neeck, SP and Shimoda, H, vol. 9241 of *Proceedings of SPIE*, SPIE, doi:10.1117/12.2073131, Conference on Sensors, Systems, and Next-Generation Satellites XVIII, Amsterdam, Netherlands, Sep 22-25, 2014, 2014.

Crutzen, P. J.: The influence of nitrogen oxides on the atmospheric ozone content, Quarterly Journal of the Royal Meteorological Society,

15   96, 320–325, doi:10.1002/qj.49709640815, http://dx.doi.org/10.1002/qj.49709640815, 1970.

Damadeo, R. P., Zawodny, J. M., Thomason, L. W., and Iyer, N.: SAGE version 7.0 algorithm: application to SAGE II, Atmospheric Measurement Techniques, 6, 3539–3561, doi:10.5194/amt-6-3539-2013, 2013.

Daumont, D., Brion, J., Charbonnier, J., and Malicet, J.: Ozone UV Spectroscopy 1. Absorption Cross-Sections at Room-Temperature, Journal of Atmospheric Chemistry, 15, 145–155, doi:10.1007/BF00053756, 1992.

20   Fishman, J., Bowman, K. W., Burrows, J. P., Andreas, R., Chance, K. V., Edwards, D. P., Martin, R. V., Morris, G. A., Pierce, R. B., Ziemke, J. R., Al-Saadi, J. A., Creilson, J. K., Schaack, T. K., and Thompson, A. M.: Remote sensing of tropospheric pollution from space, Bulletin of the American Meteorological Society, 89, 805–821, doi:10.1175/2008BAMS2526.1, 2008.

Herman, J., Cede, A., Spinei, E., Mount, G., Tzortziou, M., and Abuhassan, N.: NO2 column amounts from ground-based Pandora and MF-DOAS spectrometers using the direct-sun DOAS technique: Intercomparisons and application to OMI validation, Journal of Geophysical

25   Research-Atmospheres, 114, doi:10.1029/2009JD011848, 2009.

Hofmann, D., Bonasoni, P., De Maziere, M., Evangelisti, F., Giovanelli, G., Goldman, A., Goutail, F., Harder, J., Jakoubek, R., Johnston, P., Kerr, J., Matthews, W., McElroy, T., McKenzie, R., Mount, G., Platt, U., Stutz, J., Thomas, A., Van Roozendael, M., and WU, E.: Intercomparison of UV/Visible Spectrometers for Measurements of Stratospheric NO2 for the Network for the Detection of Stratospheric Change, Journal of Geophysical Research-Atmospheres, 100, 16 765–16 791, doi:10.1029/95JD00620, 1995.

30   Knepp, T., Pippin, M., Crawford, J., Chen, G., Szykman, J., Long, R., Cowen, L., Cede, A., Abuhassan, N., Herman, J., Delgado, R., Compton, J., Berkoff, T., Fishman, J., Martins, D., Stauffer, R., Thompson, A., Weinheimer, A., Knapp, D., Montzka, D., Lenschow, D., and Neil, D.: Estimating surface NO2 and SO2 mixing ratios from fast-response total column observations and potential application to geostationary missions, Journal of Atmospheric Chemistry, pp. 1–26, doi:10.1007/s10874-013-9257-6, http://dx.doi.org/10.1007/s10874-013-9257-6, 2015.

35   Lamsal, L. N., Krotkov, N. A., Celarier, E. A., Swartz, W. H., Pickering, K. E., Bucsela, E. J., Gleason, J. F., Martin, R. V., Philip, S., Irie, H., Cede, A., Herman, J., Weinheimer, A., Szykman, J. J., and Knepp, T. N.: Evaluation of OMI operational standard NO2 column retrievals

using in situ and surface-based NO2 observations, Atmospheric Chemistry and Physics, 14, 11 587–11 609, doi:10.5194/acp-14-11587-2014, 2014.

Malicet, J., Daumont, D., Charbonnier, J., Parisse, C., Chakir, A., and Brion, J.: Ozone UV Spectroscopy 2. Absorption Cross-Sections and Temperature-Dependence, Journal of Atmospheric Chemistry, 21, 263–273, doi:10.1007/BF00696758, 1995.

5 McKenzie, R. and Johnston, P.: Seasonal-Variations in Stratospheric NO2 at 45-degrees-S, Geophysical Research Letters, 9, 1255–1258, doi:10.1029/GL009i011p01255, 1982.

McKenzie, R., Johnston, P., Kotkamp, M., Bittar, A., and Hamlin, J.: Solar Ultraviolet Spectroradiometry in New-Zealand - Instrumentation and Sample Results from 1990, Applied Optics, 31, 6501–6509, doi:10.1364/AO.31.006501, 1992.

Newnham, D. and Ballard, J.: Visible absorption cross sections and integrated absorption intensities of molecular oxygen (O-2 and O-4), 10 Journal of Geophysical Research-Atmospheres, 103, 28 801–28 815, doi:10.1029/98JD02799, 1998.

Platt, U. and Stutz, J., eds.: Differential Optical Absorption Spectroscopy: Principles and Applications, Physics of Earth and Space Environments, Springer Verlag, 2008.

Portmann, R., Brown, S., Gierczak, T., Talukdar, R., Burkholder, J., and Ravishankara, A.: Role of nitrogen oxides in the stratosphere: A reevaluation based on laboratory studies, Geophysical Research Letters, 26, 2387–2390, doi:10.1029/1999GL900499, 1999.

15 Roscoe, H., Johnston, P., Van Roozendael, M., Richter, A., Sarkissian, A., Roscoe, J., Preston, K., Lambert, J., Hermans, C., Decuyper, W., Dzienus, S., Winterrath, T., Burrows, J., Goutail, F., Pommereau, J., D'Almeida, E., Hottier, J., Coureul, C., Didier, R., Pundt, I., Bartlett, L., McElroy, C., Kerr, J., Elokhov, A., Giovanelli, G., Ravegnani, F., Premuda, M., Kostadinov, I., Erle, F., Wagner, T., Pfeilsticker, K., Kenntner, M., Marquard, L., Gil, M., Puentedura, O., Yela, M., Arlander, D., Hoiskar, B., Tellefsen, C., Tornkvist, K., Heese, B., Jones, R., Aliwell, S., and Freshwater, R.: Slant column measurements of O3 and NO2 during the NDSC intercomparison of zenith-sky UV-visible 20 spectrometers in June 1996, Journal of Atmospheric Chemistry, 32, 281–314, doi:10.1023/A:1006111216966, 1999.

Seinfeld, J. H. and Pandas, S. N.: Atmospheric Chemistry and Physics: From Air Pollution to Climate Change, John Wiley & Sons, 1998.

Smith, W., Timofeyev, Y., and Deepak, A., eds.: Proceedings of the International Radiation Symposium (IRC, Saint Petersburg, Russia, 24-29 July 2001), 2001.

Tzortziou, M., Herman, J. R., Cede, A., Loughner, C. P., Abuhassan, N., and Naik, S.: Spatial and temporal variability of ozone and nitrogen 25 dioxide over a major urban estuarine ecosystem, Journal of Atmospheric Chemistry, 72, 287–309, doi:10.1007/s10874-013-9255-8, 2015.

Vandaele, A., Hermans, C., Simon, P., Carleer, M., Colin, R., Fally, S., Merienne, M., Jenouvrier, A., and Coquart, B.: Measurements of the NO2 absorption cross-section from 42 000 cm(-1) to 10 000 cm(-1) (238-1000 nm) at 220 K and 294 K, Journal of Quantitative Spectroscopy & Radiative Transfer, 59, 171–184, doi:10.1016/S0022-4073(97)00168-4, 4th Conference on Atmospheric Spectroscopy Applications, REIMS, FRANCE, SEP 04-06, 1996, 1998.

30 Wang, S., Pongetti, T. J., Sander, S. P., Elena, S., Mount, G. H., Cede, A., and Herman, J.: Direct Sun measurements of NO2 column abundances from Table Mountain California: Intercomparison of low- and high-resolution spectrometers, Journal of Geophysical Research-Atmospheres, 115, doi:10.1029/2009JD013503, 2010.

Wennberg, P. O., Cohen, R. C., Stimpfle, R. M., Koplow, J. P., Anderson, J. G., Salawitch, R. J., Fahey, D. W., Woodbridge, E. L., Keim, E. R., Gao, R. S., Webster, C. R., May, R. D., Toohey, D. W., Avallone, L. M., Proffitt, M. H., Loewenstein, M., Podolske, J. R., Chan, 35 K. R., and Wofsy, S. C.: Removal of Stratospheric O3 by Radicals: In Situ Measurements of OH, HO2, NO, NO2, ClO, and BrO, Science, 266, 398–404, doi:10.1126/science.266.5184.398, http://science.sciencemag.org/content/266/5184/398, 1994.

WMO: Atmospheric Ozone 1985: Assessment of our understanding of the processes controlling its present distribution and change, Volume 1, Report Number 16, Report, World Meteorological Organization, 1985.